

QENS study of methane diffusion in Mo/H-ZSM-5 used for the methane dehydroaromatisation reaction

Ian P. Silverwood, Miren Agote Arán, Ines Lezcano González, Anna Kroner, and Andrew M. Beale

Citation: [AIP Conference Proceedings](#) **1969**, 030002 (2018); doi: 10.1063/1.5039294

View online: <https://doi.org/10.1063/1.5039294>

View Table of Contents: <http://aip.scitation.org/toc/apc/1969/1>

Published by the [American Institute of Physics](#)

Articles you may be interested in

[Modelling of structure and dynamics of molten NaF using first principles molecular dynamics](#)

[AIP Conference Proceedings](#) **1969**, 030001 (2018); 10.1063/1.5039293

[Dynamics of partially folded and unfolded proteins investigated with quasielastic neutron spectroscopy](#)

[AIP Conference Proceedings](#) **1969**, 020003 (2018); 10.1063/1.5039292

[Comparative microscopic dynamics in a room-temperature ionic liquid confined in carbon pores characterized by reversible and irreversible ion immobilization](#)

[AIP Conference Proceedings](#) **1969**, 020001 (2018); 10.1063/1.5039290

[Proton dynamics of phosphoric acid in HT-PEFCs: Towards “operando” experiments](#)

[AIP Conference Proceedings](#) **1969**, 030003 (2018); 10.1063/1.5039295

[Preface: Probing Nanoscale Dynamics in Energy Related Materials - Proceedings of the Joint International Conference on Quasielastic Neutron Scattering and the Workshop on Inelastic Spectrometers \(QENS/WINS 2016\)](#)

[AIP Conference Proceedings](#) **1969**, 010001 (2018); 10.1063/1.5039289

[Molecular dynamics in 1-alkyl-3-methylimidazolium bromide ionic liquids: A reanalysis of quasielastic neutron scattering results](#)

[AIP Conference Proceedings](#) **1969**, 020002 (2018); 10.1063/1.5039291

QENS Study of Methane Diffusion in Mo/H-ZSM-5 used for the Methane Dehydroaromatisation Reaction

Ian P. Silverwood,^{1, 2, a)} Miren Agote Arán,^{2, 3,} Ines Lezcano González,^{2, 3,} Anna Kroner^{4,} and Andrew M. Beale^{2, 3}

¹ISIS Neutron and Muon Facility, Science and Technology Facilities Council, Rutherford Appleton Laboratory, Didcot, Oxfordshire, OX11 0QX, UK.

²UK Catalysis Hub, Research Complex at Harwell, Rutherford Appleton Laboratory, Didcot, Oxfordshire, OX11 0FA, UK.

³Department of Chemistry, University College London, 20 Gordon Street, London, WC1H 0AJ, UK.

⁴Diamond Light Source Ltd, Harwell Science and Innovation Campus, Didcot, Oxfordshire, OX11 0DE, UK.

^{a)}Corresponding author: ian.silverwood@stfc.ac.uk

Abstract. There is commercial interest in understanding the deactivation of Mo loaded H-ZSM-5 catalyst by coke fouling during the methane dehydroaromatization reaction (MDA). The effect of coke on methane diffusion inside the zeolite pores was studied by quasielastic neutron scattering (QENS) measurements on Mo/H-ZSM-5 samples reacted with methane for 0, 7, 25 and 60 min. Catalytic activity of the samples followed by mass spectrometry indicate that the induction period in which Mo species are carburized lasts for ~9 min; after this period the material shows selectivity to aromatics. Characterization by TGA and N₂ physisorption suggest that practically no carbon is deposited during the induction period. The ~2 wt % of coke formed after one hour of reaction has a negligible effect in the zeolite crystal structure but a small effect on the micropore volume. The QENS studies show that the methane transport by jump diffusion is however not measurably affected by the accumulated coke in the samples.

INTRODUCTION

The effects of carbonaceous deposits, or “coke”, on catalyst performance have been extensively studied over the past decades with the principle focus on the role of coke in catalyst deactivation. Possible deactivation pathways of supported metal catalysts due to fouling by carbon or coke are: the formation of a chemi- or physisorbed carbon layer blocking reactant access to reactive surface sites, the total encapsulation of a metal particle and, in case of porous catalysts such as zeolites, the plugging of micro- and mesopores such that access of reactants to the pores is denied [1]. In extreme cases, carbon filaments may build up in pores to the extent that they stress and fracture the material, ultimately causing the loss of structure [1]. There is a strong commercial need to understand the mechanisms by which coke causes a catalyst deactivation; costs to industry for material replacement and reactivation total billions of dollars per year and in many cases, such as in the methane dehydroaromatization reaction, it compromises the industrialization of the process.

MDA is a promising route to replace the depleting fossil fuels with methane as the precursor for obtaining commodity chemicals. It consists of a non-oxidative reaction that converts methane directly into C₂, C₃ fractions and especially benzene giving hydrogen as a co-product. The only commercialized routes for the valorisation of methane nowadays require the formation of syngas followed by the synthesis of methanol or dimethyl ether; these are multi-step routes which are energy intensive and economically expensive. MDA is attractive for being a one-step direct route to the formation of benzene, also a key precursor to the manufacture of chemicals. The most common catalytic material for MDA is Mo-containing H-ZSM-5 which is considered a bifunctional catalyst where Mo carbides and

zeolite Brønsted acid sites (BAS) play a catalytic role. It has been proposed that the molybdenum carbide phase that is formed during carburization of molybdenum oxide species converts methane into ethylene; Brønsted acid sites of the zeolite convert ethylene to benzene and other aromatics [2]. In spite of the promising catalytic activity of this material, the formation of carbon deposits and rapid deactivation of the catalyst is an obstacle for its industrial application. Much effort has been devoted to understand the effect of coke on the Mo/H-ZSM-5 deactivation. Although it is proposed that the presence of coke may have positive effect and a catalytic role in MDA [3, 4], there is a consensus that the extensive formation of carbon deposits during prolonged reaction times is one of the main causes of deactivation. Debate is ongoing regarding the nature and location of coke, some groups have concluded that carbon deposition occurs mainly on molybdenum sites present on the external surface of H-ZSM-5 [5], in this case deactivation of the catalyst would occur mainly due to the coverage of Mo sites responsible for methane activation. Other studies report that deactivation is caused by polyaromatic type of carbon formed at the Brønsted acid sites (BAS) located on the external surface of the zeolite crystals [6, 7]. It is suggested that these carbon species eventually cover the zeolite pore apertures [8, 9] impeding the access of the methane into Mo active sites inside pores. Nevertheless, zeolite surface silylation studies show that the coverage of the BAS inside the micropores by carbonaceous species also contributes to catalyst deactivation [10]. Hensen et al. proposed a combined effect mechanism in which carbon deposit formation induces deactivation of the catalyst by blocking the accessibility to BAS in the zeolite micropores as well as by promoting the sintering of Mo carbide active sites [11].

Several approaches have proved to increase the MDA catalytic lifetime. Research done in catalyst formulation suggests that zeolites with large cages such as MCM-22 afford a higher coke accommodation resulting in a greater tolerance to carbonaceous deposits [12]. Engineering approaches include the design of reactor configurations to regenerate the carbon-containing catalyst by the use of optimized O₂ pulses [13]. The addition of hydrogen or oxidants (e.g. CO₂) as well as C₂–C₄ alkanes/alkenes to the methane feed can also improve catalyst longevity [14]. Nevertheless, deactivation by coking cannot be completely suppressed in MDA and is still the main handicap for the commercialization of the route.

A detailed understanding of the fouling mechanism by coke in MDA is essential for the development of durable catalysts formulations or engineering approaches to cope with rapid deactivation. In the present study, we perform quasi elastic neutron scattering (QENS) studies to get insight into the extent of pore blocking during the reaction and its effect in methane diffusion inside micropores. The speed of the diffusion of the reactive guest molecules to the catalytic site plays a big part in its activity and the product selectivity is often diffusion controlled. Understanding the dynamics of methane in the reacted catalysts containing carbon deposits will help us to discern between the possible deactivation mechanisms.

METHOD

Catalyst synthesis

NH₄-ZSM-5 with Si/Al ratio of 15 was purchased from Zeolyst (product code CBV 3024E). 4 wt. % Mo/H-ZSM-5 catalyst was prepared by solid state ion exchange: MoO₃ (99.97%, Sigma Aldrich) and the zeolite were mechanically mixed in an agate mortar for 30 min followed by calcination at 973 K for 30 min under O₂/He flow (20 vol% O₂ in He) ramping at 10 K/min.

Catalytic reaction

The reactions were carried out at 950 K using a GHSV of 750.6 h⁻¹. 4 g of catalyst was introduced to a tubular quartz reactor with an internal diameter of 2 cm. The catalyst was supported on quartz wool in the isothermal zone of the oven; the bed length was ~2 cm. All gases were fed using thermal mass flow controllers. The catalyst was first activated by increasing the temperature at a rate of 10 K/min to 973K in an O₂/He (20 vol% O₂ in He) gas flow of 78.5 ml/min. The temperature was held at 973 K for 30 min and then reactor feed was switched to pure Ar, keeping the same total flow rate and temperature, to flush the lines from oxidising gases. Finally, the MDA reaction was started by switching the reactor feed to a CH₄/Ar mixture (50 vol% CH₄ in Ar). Products were analysed by an online mass spectrometer (Pfeiffer-Omnistar-GSD-301-T3). To follow the reaction process, samples were recovered after calcination and after 7, 25 and 60 minutes of reaction under methane. The catalyst recovery was carried out by cooling the reactor under flowing Ar, the samples were then collected from the reactor in air.

QENS Measurement

Reacted samples were dried overnight at 423 K in copper-sealed steel tubes with CF flanges attached to a turbomolecular pump, before being sealed and cooled. Thereafter they were transferred into indium-sealed aluminium sample holders that provided annular spacing of 2 mm thickness and held approximately 3.5 g of sample in an Ar-filled glovebox. These sample holders were fitted with a bellows valve so the samples could be attached to suitable gas handling apparatus to allow control of the atmosphere surrounding the sample whilst positioned in the neutron beam. Neutron scattering data was collected from the evacuated samples, then dosed at room temperature to 1 bar methane. A 1 l buffer volume was included to account for volumetric changes due to temperature and ensure saturation of the zeolite. Spectra were recorded on the IRIS spectrometer at the STFC ISIS neutron and muon facility using the (002) reflection of the pyrolytic graphite analyser. Temperature was controlled between 10 and 300 K with a helium closed-cycle refrigerator. Data reduction and analysis used a combination of Mantid [15] and DAVE [16].

Characterisation

Weight-loss curves were obtained from thermogravimetric analysis (TGA) using a TA Q50 apparatus. Samples were placed in a Pt sample pan and heated at a rate of 5 K/min to 1073 K under an artificial air flow of 60 mL/min. Nitrogen sorption isotherms were measured at 77 K on a Quadrasorb EVO instrument Model QDS-30. The samples were outgassed at 623 K overnight under high vacuum prior to the sorption measurements. The Brunauer–Emmett–Teller (BET) equation was used to calculate the specific surface area in the pressure range $p/p_0 = 0.05\text{--}0.25$. The micropore volume was calculated from the t-plot curve using the thickness range between 3.5 and 6 Å.

RESULTS

Reaction

Figures 1 and 2 show the time resolved mass spectrometry (MS) data obtained during reaction. All the data shown was normalized to the Ar signal. Figure 1 corresponds to MS signal of combustion products (H_2O , CO and CO_2) which are formed during the induction period in the initial minutes of the reaction. This data presents an initial spike of CO and CO_2 from 0–2 min time on stream followed by a decrease in the detected signal between 2–4 min. This is followed by a second spike between 4–9 min after which the signals for these two components decrease drastically. The response for CH_4 by contrast climbs in intensity up to 4 min, but is followed by a significant decrease and by an upturn in signal intensity between 9 and 15 min. Between 15–60 min the signal for CH_4 reaches a plateau. Previous operando X-ray emission spectroscopy studies report that the first peak of combustion products is due to partial carburization of MoO_3 into MoC_xO_y intermediate species while the second peak of combustion corresponds to further carburization of molybdenum species to Mo_2C [2].

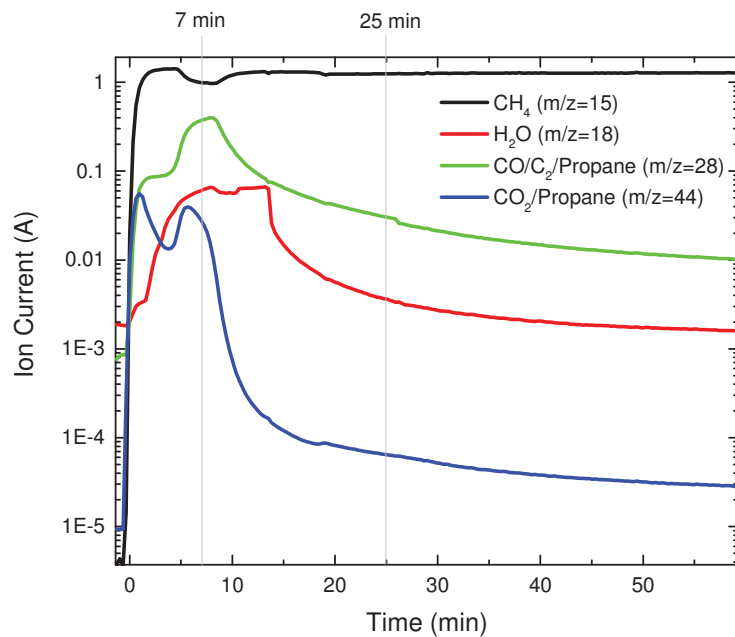


FIGURE 1. Mass spectrometry traces of CH_4 and oxidised reaction products formed during the MDA reaction on Mo/H-ZSM-5 (4 wt. %, Si/Al=15) at 973 for 60 min.

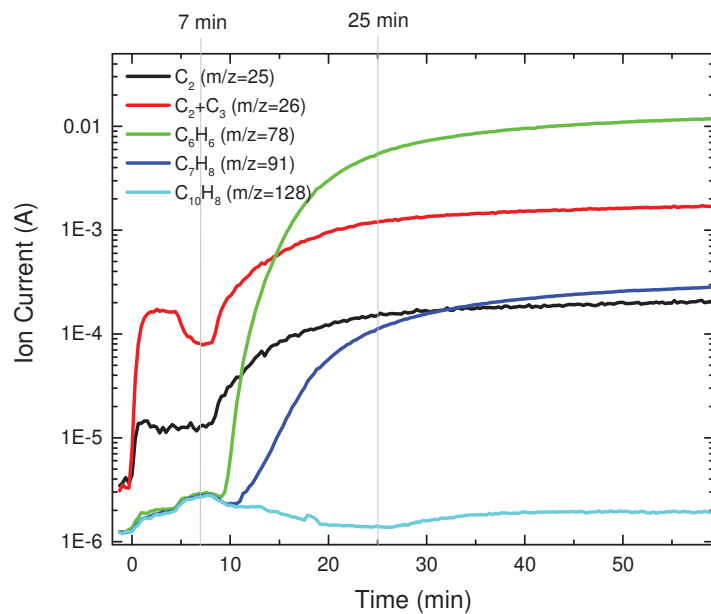


FIGURE 2: Mass spectrometry traces of hydrocarbon products formed during the MDA reaction on Mo/H-ZSM-5 (4 wt. %, Si/Al=15) at 973 K for 60 min.

Characterisation

TGA was employed to characterize the carbonaceous deposits on the spent catalysts. The recorded profiles for the catalyst after calcination (0 min) and after 7, 25 and 60 minutes of reaction are shown in Fig. 3. The weight loss before 550 K is attributed to desorption of the water, which is adsorbed when the samples are exposed to air after the reaction. For the samples reacted for 25 and 60 min a slight weight increase is observed in the range of 550–700 K which is attributed to the reaction between oxygen and Mo-carbides formed [17]. The sample reacted for 7 min show no mass gain which is explained by the lower extent of carburization of the Mo species during the induction period.

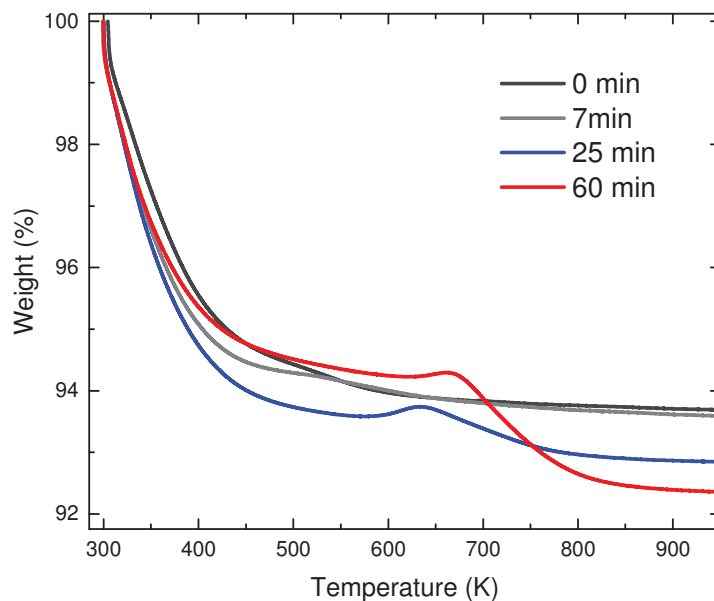


FIGURE 3: Weight-loss curves of activated and spent Mo/H-ZSM-5 zeolites.

The decrease of weight from 620 to 900 K is caused by the burning-off of the coke. In their catalyst deactivation studies for Mo/H-ZSM-5, Hensen et al. distinguished three types of carbon deposits as a function of the calcination temperature [11]. These included light carbonaceous species associated with Mo carbides (~693 K), soft coke thought to be amorphous in nature and likely formed in the proximity of Mo-carbide particles (~753 K) and hard coke mainly comprised of PAHs formed by reactions of olefins on BAS located at the external surface of the zeolite (~813 K). The results shown in table 1 suggest that there is an accumulation of carbon deposits over time, up to 1.9 wt % after one hour of reaction. These deposits are burned-off from 630 K to 800 K suggesting that the deposits formed correspond to soft coke and carbonaceous species associated with Mo-carbides.

TABLE 1. Mass loss of the spent Mo/H-ZSM-5 catalysts determined by TGA.

Sample	Total mass loss (wt %)	Mass loss (wt %)	
		T < 550 K	T 600 to 900 K
Mo/H-ZSM-5 0 min	6.3	5.6	
Mo/H-ZSM-5 7 min	6.4	5.7	
Mo/H-ZSM-5 25 min	7.1	6.4	0.8
Mo/H-ZSM-5 60 min	7.6	5.8	1.9

Table 2 lists the textural properties of the catalysts. The decrease in the micropore volume upon activation by calcining at 973 K indicates that a fraction of the Mo phase is located in the zeolite micropores [18]. The catalyst after calcination and after 7 and 25 min of reaction, all had comparable micropore area. There is a small drop in the surface area and micropore volume for the sample reacted for 60 min indicating that carbon deposits start to fill or cover the pores. Nevertheless, this drop is rather small and it may indicate that the majority of carbon deposits are being formed in the sample periphery. This is in agreement with fluorescence-lifetime images we have previously reported for Mo/H-ZSM-5 catalysts after 70 minutes reaction under very similar reaction conditions. [2]

TABLE 2. Textural properties of fresh and spent Mo/H-ZSM-5.

Sample	S_{BET} (m^2/g)	S_{micro} (m^2/g)	S_{external} (m^2/g)	V_{micro} (cc/g)
H-ZSM-5	412	344	38	0.151
Mo/H-ZSM-5 0min	344	285	59	0.117
Mo/H-ZSM-5 7min	351	292	59	0.122
Mo/H-ZSM-5 25min	360	302	58	0.125
Mo/H-ZSM-5 60min	319	274	46	0.109

Neutron Diffraction

Figure 4 shows the neutron diffraction patterns acquired at 300 K for a series of samples as a function of reaction time, with and without the presence of dosed CH_4 . All samples correspond to the H-ZSM-5 crystal structure. The highest intensity reflections in the diffractograms appear with d spacings of 3.8658, 3.8328, 3.7333 and 3.6607 Å which correspond to the (5,1,0), (0,5,1), (6,0,3) and (1,3,3) reflections respectively. The intensity of all reflections remains constant across all samples studied, in addition no obvious shift in reflection position or reflection broadening is seen to occur. This indicates that the zeolite structure was maintained under reaction conditions without being notably affected by zeolite de-alumination, the presence of adsorbed methane, or by the presence of coke; it is likely however, that any carbon deposits present will be amorphous. Nevertheless, the absence of extra reflections suggests that no large MoO_3 crystallites were present after calcination, and there is no evidence for significant quantities of Mo_2C or $\text{Al}_2(\text{MO}_4)$ being formed during these early stages of reaction.

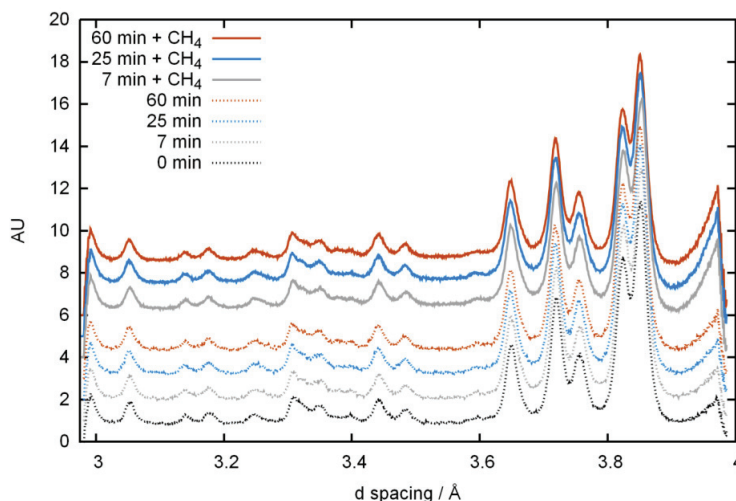


FIGURE 4: Neutron diffraction from 4% Mo/H-ZSM-5 catalysts used in the MDA reaction. The uppermost diffraction patterns correspond to samples containing adsorbed methane.

QENS

The IRIS instrument has 51 detectors that cover a range of 25-160° associated with the graphite analyser. For data analysis these may be grouped together at the expense of resolution in Q to increase the signal to noise ratio and decrease collection time. Figure 5 displays the data recorded at 300 K summed across all detectors. At the peak centre, there is virtually no difference in intensity between the methane loaded samples and those without. However, changes can be seen between samples coked for different periods. This illustrates that there is more elastic scatter with increased reaction time, which was attributed to immobile coke deposits. In the wings of the peak, there is an obvious discrepancy between the methane-loaded samples and those without, demonstrating that the methane is mobile. However, the level of coking does not seem to affect the mobility of the methane, as the wings of the peaks from the loaded samples are closely matched. A subtle broadening of the unloaded samples is present with increased reaction time, suggesting that the coke deposits are associated with a minority mobile species.

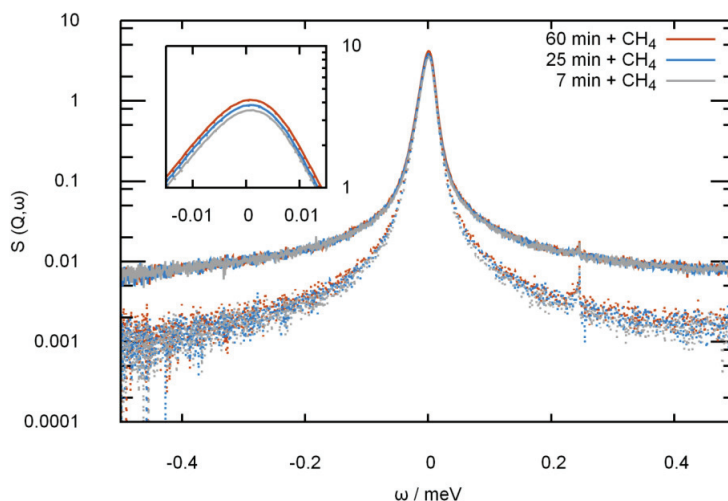


FIGURE 5: Quasielastic peak for samples summed across all detectors. Solid lines indicate the coked samples loaded with methane, dashed lines indicate them without. Inset shows detail of peak maximum.

The Q -resolved data from methane collected at 300 K adsorbed on Mo/H-ZSM-5 after 25 minutes reaction is presented in Fig. 6. Bragg peaks are readily apparent due to the high crystallinity of the H-ZSM-5 across a wide Q range, and need to be compensated for in the data analysis. To obtain a corrected measurement for the methane diffusion, the unloaded samples were fitted to a delta function convoluted with an experimentally determined resolution function. The methane data was fitted to a convolution of a delta, a Lorentzian and the same resolution. The elastic scatter from the methane was then calculated by subtracting the delta function of the unloaded coked zeolite from the corresponding loaded sample. This process provided reasonable fitting at low Q , although failed at higher Q values. Figure 7 displays the variation in the width of the Lorentzian function for the coked samples at low Q , fitted to the Chudley-Elliott jump diffusion model.

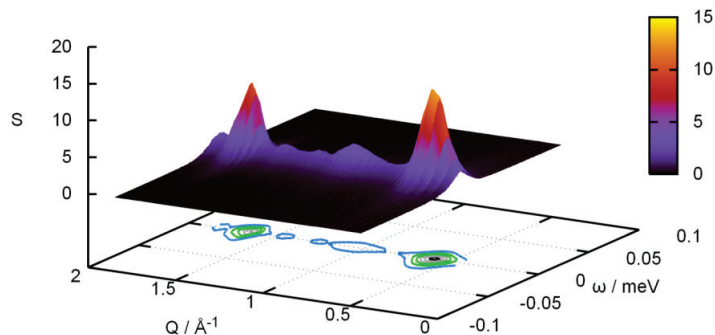


FIGURE 6: Neutron scattering data for methane adsorbed on Mo/H-ZSM-5 after 25 min reaction.

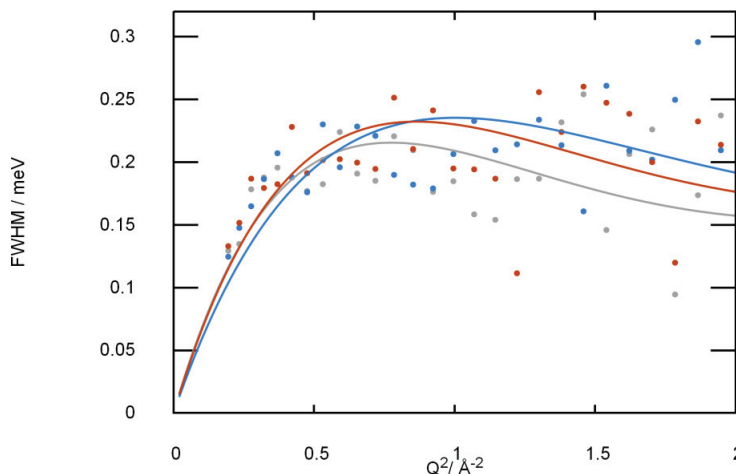


FIGURE 7: Quasielastic peak width for methane adsorbed on Mo/H-ZSM-5. Lines correspond to data fitting to the Chudley-Elliott model.

CONCLUSIONS

Mo/H-ZSM-5 catalysts reacted for 0, 7, 25 and 60 minutes have been studied. Neutron diffraction patterns indicate that the zeolite framework does not undergo changes during the course of the reaction. One hour of reaction results in the formation of 2 wt% of coke that does not greatly affect the micropore volume of the samples. Regarding methane transport inside zeolite pores, jump diffusion has previously been shown to be the mechanism of transport for methane in H-ZSM-5 [19, 20] on the length scales probed by QENS. The diffusion of methane in our samples does not appear strongly affected by the presence of the deposited coke. The strength of scattering between the samples suggests that similar numbers of mobile scatterers are observed in the beam, which suggests that access to the pore network is not significantly retarded by the reaction coke. Whilst it is possible that there is coke that alters diffusion over longer distances, the results suggest that the reactant is free to access the active sites inside the zeolite bulk. This implies that carbon deposits present in quantities as great as ~ 2 wt. % do not dramatically affect methane mass transport suggesting a certain tolerance of these catalysts to carbon fouling.

ACKNOWLEDGEMENTS

Experiments at the ISIS Pulsed Neutron and Muon Source were supported by a beamtime allocation from the Science and Technology Facilities Council (RB 1610479). Miren Agote-Aran acknowledges financial support from a UCL Impact PhD award, Diamond Light Source and Johnson Matthey Plc.

REFERENCES

1. M.D. Argyle and C.H. Bartholomew, *Catalysts* **5**, 145–269 (2015).
2. I. Lezcano-Gonzalez, R. Oord, M. Rovezzi, P. Glatzel, S.W. Botchway, B.M. Weckhuysen and A.M. Beale, *Angew. Chem. Int. Ed.* **55**, 5215–5219 (2016).
3. D. J. Wang, J. H. Lunsford and M. P. Rosynek, *J. Catal.* **169**, 347–358 (1997).
4. C. H. Collett and J. McGregor, *Catal. Sci. Technol.* **6**, 363–378 (2016).
5. J. Shu, A. Adnot and B. P. A. Grandjean, *Ind. Eng. Chem. Res.* **38**, 3860–3867 (1999).
6. T. Behrsing, H. Jaeger and J.V. Sanders, *Appl. Catal.* **54**, 289–302 (1989).
7. W.P. Ding, G.D. Meitzner and E. Iglesia, *J. Catal.* **206**, 14–22 (2002).
8. J. Bai, S. Liu, S. Xie, L. Xu and L. Lin, *Catal. Lett.* **90**, 123–130 (2003).
9. J. Bai, S. Lie, S. Xie, L. Xu and L. Lin, *React. Kinet. Catal. Lett.* **82**, 279–286 (2004).
10. D. Ma, Y. Shu, M. Cheng, Y. Xu and X. Bao, *J. Catal.* **194**, 105–114 (2000).
11. C.H.L. Tempelman and E.J.M. Hensen, *Appl. Cat. B: Environ.* **176**, 731–739 (2015).
12. D. Ma, Y. Y. Shu, X. W. Han, X. M. Liu, Y. D. Xu and X. H. Bao, *J. Phys. Chem. B* **105**, 1786–1793 (2001).
13. N. Kosinov, F.J.A.G. Coumans, E. Uslamin, F. Kapteijn and E.J.M. Hensen, *Angew. Chem. Int. Ed.* **55**, 15086–15090 (2016).
14. J.J. Spivey and G. Hutching, *Chem. Soc. Rev.* **43**, 792–803 (2014).
15. H. Arnold, J.C. Bilheux, J.M. Borreguero, A. Buts, S.I. Campbell *et al.* *Nucl. Instrum. Meth. A* **764**, 156–166 (2014).
16. R.T. Azuah, L.R. Kneller, Y. Qiu, P.L.W. Tregenna-Piggott, C.M. Brown, J.R.D. Copley, and R.M. Dimeo, *J. Res. Natl. Inst. Stan.* **114**, 341–358 (2009).
17. H. Liu, L. Su, H. Wang, W. Shen, X. Bao and Y. Xu, *App. Cat A: Gen.* **236**, 263–280 (2002).
18. Y. Shu, D. Ma, L. Xu, Y. Xu and X. Bao, *Catal. Lett.* **70**, 67–73 (2000).
19. H. Jobic, M. Bée, and G. J. Kearley, *Zeolites* **9**, 312–317 (1989).
20. H. Jobic, M. Bée, J. Caro, M. Bülow and J. Kärger, *J. Chem. Soc. Faraday Trans. 1* **85**, 4201–4209 (1989).